Graphical abstract

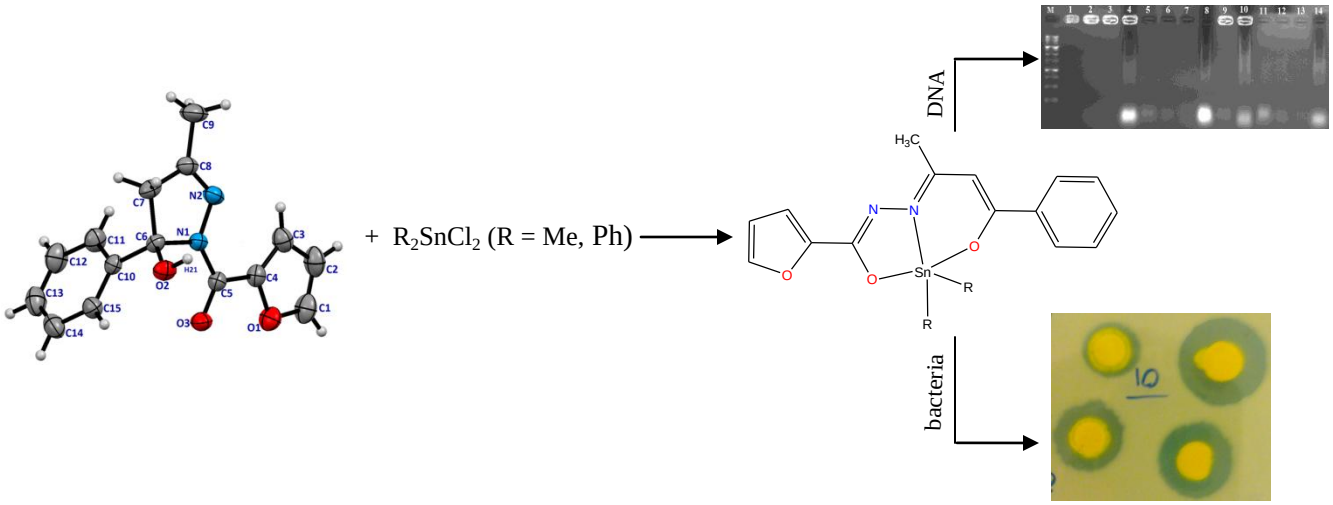

doi:10.1016/j.jorganchem.2015.06.034

Graphical abstract

Diorganotin(IV) complexes with 2-Furancarboxylic acid hydrazone derivative of benzoylacetone: Synthesis, X-ray structure, antibacterial activity, DNA cleavage and molecular docking

Tahereh Sedaghat, Yahya Ebrahimi, Lucia Carlucci, Davide M. Proserpio, Valiollah Nobakht, Hossein Motamedi, Mohammad Reza Dayer

Two new diorganotin(IV) complexes have been synthesized with a hydrazone derived from furan-2-carbohydrazide and benzoylacetone and characterized both in solid and solution. **A**ntibacterial activity, DNA cleavage and molecular docking have been studied.

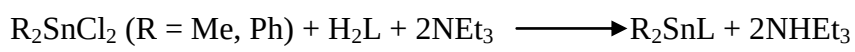

Diorganotin(IV) complexes with 2-furancarboxylic acid hydrazone derivative of benzoylacetone: Synthesis, X-ray structure, antibacterial activity, DNA cleavage and molecular docking

Tahereh Sedaghat[a*], Yahya Ebrahimi[a], Lucia Carlucci[b], Davide M. Proserpio[b,c], Valiollah Nobakht[a], Hossein Motamedi[d], Mohammad Reza Dayer[d]

[a]*Department of Chemistry, College of Sciences, Shahid Chamran University, Ahvaz, Iran*

[b]*Dipartimento di Chimica, Università degli Studi di Milano, Via C. Golgi 19, 20133, Milano, Italy*

[c] *Samara Center for Theoretical Materials Science (SCTMS) Samara State University, Samara 443011, Russia*

[d]*Department of Biology, College of Sciences, Shahid Chamran University, Ahvaz, Iran*

**Corresponding author: tsedaghat@scu.ac.ir , Fax: 98 611 3331042*

Abstract

Two new diorganotin(IV) complexes, Me_2SnL and Ph_2SnL, have been synthesized from the reaction of Me_2SnCl_2 and Ph_2SnCl_2 with the hydrazone H_2L [H_2L = (Furan-2-yl)(5-hydroxy-3-methyl-5-phenyl-4,5-dihydro-1*H*-pyrazol-1-yl)-methanone] derived from furan-2-carbohydrazide and benzoylacetone. The new compounds have been characterized by elemental and spectroscopic analyses. The crystal structures of the monohydrate form of the ligand and of the Me_2SnL derivative have been also determined by X-ray crystallography. Experimental evidences confirm the existence of the hydrazone ligand exclusively in cyclic form in both solution and solid state. On coordination to tin the hydrazone undergoes a ring opening reaction and a doubly deprotonation to act as a tridentate ligand via imine nitrogen and enolic oxygens. The tin atom in the complexes is five coordinate with geometry between square-pyramidal and trigonal-bipyramidal. The *in vitro* antibacterial activity of ligand and its complexes has been evaluated against Gram-positive (*Bacillus subtilis* and *Staphylococcus aureus*) and Gram-negative (*Escherichia coli* and *Pseudomonas aeruginosa*) bacteria. The interaction between compounds with bacterial DNA was also studied by molecular docking. Our findings indicate that diphenyltin(IV) complex, by binding to DNA via minor groove to TATA sequence in genes upstream, has good activities along with the standard antibacterial drugs. Our agarose-gel electrophoresis experiments show that the ligand exert DNA cleavage, while Me_2SnL and Ph_2SnL did not.

Keywords: Organotin(IV), Hydrazone, Diketone, Antibacterial activity, DNA cleavage, Molecular docking

Introduction

1,3-Diketones constitute an important class of compounds, which is used in organic chemistry for the synthesis of heterocycles [1, 2] and in coordination chemistry as ligand [3]. Moreover, Imines (Schiff bases) can be obtained from condensation of these dicarbonyl compounds and primary amines. The derived Schiff bases have keto-enol tautomerism with strong intramolecular hydrogen bonds (N–H…O or N…H–O). They are of biological interest, play as synthetic intermediates in organic reactions and act as sensor materials [4-6]. These compounds can also be used as coordination ligands for transition and non-transition metals; however, less attention has been paid to this type of systems. Recently we have reported synthesis, structural and theoretical studies and antibacterial activities of several Schiff bases derived from condensation of β-diketones with aminophenol derivatives and their complexes with transition metals and organotins [7-12]. In continuation of our earlier work, we are herein reporting a hydrazonic derivative of a 1,3-diketone and its organotin(IV) complexes. Hydrazone-based Schiff base ligands, and their metal complexes have received much attention because of their potential pharmacological applications [13, 14]. Facile keto-enol tautomerization and the availability of several potential donor sites in these ligands allows and encourages chemists to construct complexes with large structural varieties [15]. Along this line, organotin(IV) complexes of hydrazones have received considerable attention for both structural and biological importance: many of these compounds may interact with biological systems in different ways as bactericides, fungicides, acaricides and industrial biocides [16-21]. Recently these compounds have been used in new contexts as in cancer chemotherapy [22, 23]. In view of a few reports on organotin(IV) complexes of hydrazones derived from 1,3-diketones [24-28], it was considered worthwhile to investigate the synthesis, structural aspects and biological properties of hydrazonic derivatives of

1,3-diketones and their organotin complexes. In the present paper, 2-furancarboxylic acid hydrazone derivative of benzoyl acetone and its dimethyl- and diphenyltin complexes have been synthesized. The solution and solid state structures as well as biological properties of ligand and complexes are reported. In order to elucidate the interaction mechanisms for these compounds, we performed *In Silico* experiments using molecular dynamic and docking.

2. Experimental

2.1. Materials and methods

All starting materials were purchased from Merck while diphenyltin dichloride was supplied from Acros Company and were all used as received. All solvents were of reagent grade and used without further purification. IR spectra were obtained using a FT BOMEM MB102 spectrophotometer. The ^{1}H, ^{13}C and ^{119}Sn NMR spectra were recorded with Bruker Avance Ultrashield spectrometers using TMS and $SnMe_4$ as references, respectively.

*2.2 Synthesis of the ligand (**1**)*

A solution of furan-2-carbohydrazide (0.630 g, 5 mmol) and benzoylacetone (0.81 g, 5 mmol) in ethanol (30 mL) was refluxed for 4 h. Cubic white single crystals were obtained after standing the solution for 3 days at room temperature (**1a**). Yield: 1.152 g (80 %), m.p. 128-132 ^{0}C; Anal. Calcd. For $C_{15}H_{14}N_2O_3$: C, 62.49; H, 5.59; N, 9.71; Found: C, 62.22; H, 5.61; N, 9.83; FT-IR (KBr, cm^{-1}): ν(OH), 3396; ν(C=O), 1640; ν (C=N), 1626; ν(CH_2), 1434; ν(C-O), 1318; ν(OH), 1163; ^{1}H NMR (250 MHz, $CDCl_3$): δ = 2.16 (s, 3H, H_9), 3.00 (d, 1H, H_7, $^{2}J_{HH}$ =18.7 Hz), 3.34 (d, 1H, H_7, $^{2}J_{HH}$ = 18.7 Hz), 5.30 (s, 1H, OH), 6.57 (m, 1H, H_2), 7.30 (d, 1H, H_3, $^{3}J_{HH}$ = 4.0 Hz), 7.32 - 7.46 (m, 4H, H_1, 3ArH), 7.62 (m, 2H, 2ArH) (See Figure 3 for numbering). Synthesis of **1**

in methanol gives the hydrated form of this compound as bright yellow crystals suitable for X-ray crystallography (**1b**).

*2.3. Synthesis of Me_2SnL (**2**)*

H_2L (0.067 g, 0.25 mmol) was dissolved in ethanol (5 mL) and triethylamine (0.5 mmol) was added. This solution was stirred for 30 min and then $SnMe_2Cl_2$ (0.055 g, 0.25 mmol) in ethanol (5 mL) was added. The mixture was refluxed for 2 h. The yellow-orange crystals suitable for X-ray crystallography were obtained after standing the solution for 2 days at room temperature. Yield: 0.337 g (81%); m.p. 147-150 $^{\circ}$C; Anal. Calcd. For $C_{17}H_{18}N_2O_3Sn$: C, 48.95; H, 4.35; N, 6.71 %. Found: C, 48.62; H, 4.78; N, 6.69; FT-IR (KBr, cm^{-1}): ν(C=N), 1596; ν(C=N), 1586; ν_{as}(Sn-C), 597; ν(Sn-O), 551; ν_s(Sn-C), 522; ν(Sn-N), 456; ^{1}H NMR (250 MHz, $CDCl_3$): δ = 0.83 [s, 6H, $SnMe_2$, $^2J(^{117/119}Sn\text{-}^1H)$ = 75.3/78.8 Hz]; 2.55 (s, 3H, H_{17}); 5.66 (s, 1H, H_7); 6.50 (m, 1H, H_1); 6.98 (dd, 1H, H_3, $^3J_{HH}$ = 3.5, $^4J_{HH}$ = 0.75 Hz); 7.39-7.45 (m, 3H, $H_{11,12,13}$); 7.54 (m, 1H, H_2); 7.77-7.81 (m, 2H, $H_{10,14}$); ^{13}C NMR (62 MHz, $CDCl_3$): δ = 1.38, $C_{15,16}$; 23.75, C_{17}; 94.43, C_7; 111.48, C_3; 111.97, C_1; 126.59, $C_{11,13}$; 128.30, $C_{10,14}$; 130.35, C_{12}; 138.68, C_9; 143.98, C_2; 148.63, C_4;157.92, C_5; 170.05, C_6; 174.00, C_8.; ^{119}SnNMR (111 MHz, $CDCl_3$): δ = -149.5 (See Figure 5 for numbering).

*2.4. Synthesis of Ph_2SnL (**3**)*

To solution of ligand (0.067 g, 0.25 mmol) in ethanol (5 ml), triethylamine (0.5 mmol) was added. This solution was stirred for 30 min and then Ph_2SnCl_2 (0.085 g, 0.25 mmol) in ethanol (5 ml) was added. The reaction mixture was refluxed for 3h. A yellow precipitate was formed which was filtered, washed with ethanol and dried over $CaCl_2$. Yield: 0.411 g (76%); m.p. 169-

173 °C; Anal. Calcd. For $C_{27}H_{22}N_2O_3Sn$: C, 59.92; H, 4.09; N, 5.17 %. Found: C, 59.97; H, 4.42; N, 5.32; FT-IR (KBr, cm^{-1}): ν(C=N), 1596; ν(C=N), 1587; ν(Sn-O), 544; ν(Sn-N), 458; ^{1}H NMR (250 MHz, $CDCl_3$): δ = 2.57 (s, 3H, H_{17}); 5.83 (s, 1H, H_7); 6.57 (m, 1H, H_1); 7.17 [(d, 1H, J = 3.25 Hz, H_3]; 7.40-7.46 [m, 6H. $H_{m,p}(Ph_2Sn)$]; 7.52 (m, 3H, $H_{11,12,13}$); 7.60 (m, 1H, H_2); 7.85-7.90 [m, 4H, $H_o(Ph_2Sn)$]; 7.99-8.03 (m, 2H, $H_{10,14}$); ^{13}CNMR ($CDCl_3$): δ = 23.90, C_{17}; 95.22, C_7; 111.54, C_3; 112.96, C_1; 126.73, $C_{11,13}$; 128.56, $C_{10,14}$; 128.86, C_m [$^3J(^{119}Sn–^{13}C)$ = 85.6 Hz]; 130.39, C_p [$^2J(^{119}Sn–^{13}C)$ = 17.3]; 130.67, C_{12}; 136.10, C_o [$^2J(^{119}Sn–^{13}C)$ = 54.3]; 138.24, C_9; 139.52, C_i; 144.31, C_2; 148.58, C_4; 156.35, C_5; 170.15, C_6; 174.05, C_8; ^{119} Sn NMR (111 MHz, $CDCl_3$): δ= -325.1(See Figure 5 for numbering).

2.5. X-ray crystal structure determination

X-ray data were collected on a Bruker Apex II diffractometer using MoKα radiation. The structures were solved using direct methods and refined using a full-matrix least squares procedure based on F^2 using all data [29]. Hydrogen atoms were placed at geometrically estimated positions. Details relating to the crystals and the structural refinements are presented in Table 1. Full details of crystal data and structure refinements, in CIF format, are available as Supplementary Materials.

2.6. Antibacterial tests

The in vitro antibacterial activity of ligand and its corresponding organotin(IV) complexes was studied against two Gram-positive (*Bacillus subtilis* ATCC 6633 and *Staphylococcus aureus* ATCC 6538) and two Gram-negative (*Escherichia coli* ATCC 25922 and *Pseudomonas aeruginosa* ATCC 9027) bacteria in Kirby-Bauer disc diffusion test according to the CLSI

standard protocols [30]. For this purpose, the test species were cultured in Muller-Hinton broth (Merck, Germany) and incubated at 37°C till 0.5 McFarland turbidity was obtained. A lawn culture was then prepared on Muller-Hinton agar (Merck, Germany) plates using sterile cotton swabs. The compounds were dissolved in $CDCl_3$ at 10, 20, 40 and 80 mg/mL concentration and sterile blank discs (6.4 mm diameter) were saturated by these solutions. So, the final effective dose per disc was 0.4, 0.8, 1.6 and 3.2 mg. These discs were left for 15min at room temperature and then placed on lawn cultures. A blank disc saturated with $CDCl_3$ was also prepared for each bacterial species and used as a control for solvent. The plates were incubated at 37 °C for 24 h. The inhibition zone diameters around each disk were measured in mm. In order to compare the results, the effect of standard antibiotic discs including Vancomycin, Streptomycin, Penicillin, Nalidixic acid and Gentamicin were studied as previously mentioned.

2.7. Gel electrophoresis assay

The bacterial DNA was extracted by boiling method [31]. For this purpose, 1mL of bacterial suspension was centrifuged at 10000 rpm for 10 min. The precipitate was dissolved in 1 mL of sterile distilled water and boiled for 15 min at 100°C. A centrifuge at 5000 rpm for 1 min was then performed and the supernatant was harvested. Cold ethanol was added to this supernatant at 2.5 V/V and remained overnight at -20°C. The DNA was precipitated by centrifugation at 13000 rpm for 10min. Finally the precipitate was dissolved in 100 µL of DNase free sterile water. DNA was stored at -20°C till experiments. A 20 mg/mL solution of each compound in $CHCl_3$ was prepared and 100 µL of this solution was mixed with 100 µL of DNA solution and incubated at 37 °C for 2h. A positive control was prepared through mixing 100 µL of H_2O_2 with 100 µL of DNA and treated as same as previously described. Furthermore, an untreated DNA was regarded

as negative control. For finding if the DNA was affected by compounds, agarose gel electrophoresis was performed. One percent agarose was prepared in TAE buffer and boiled. DNA safe stain was added to the gel and poured in horizontal electrophoresis tray 0.5 μL of each treated DNA was mixed with 2μL of loading dye and loaded in agarose gel. A 1Kb DNA ladder was also loaded in a well. Electrophoresis was done at 100 V for 50 min. The gel was documented under UV irradiation by UVI/TEC gel documentation.

2.8. Molecular Dynamic and Docking experiment

In order to study the expected interactions between H_2L, Me_2SnL and Ph_2SnL with bacterial DNA, we constructed 24 base pair DNA in HyperChem software with three different zone of an AT rich region with 8 base pair that mimic TATA box, a GC rich region with 8 base pair that mimic GC region both found in upstream of promoter region of genes, and an intervening region composed of two successive AGTC box (8 base pair). This region mimics a regular portion of DNA in eukaryotic or prokaryotic cells. The DNA was placed in rectangular cubic box with dimensions of 3.79×12.76×5.02 nanometers and filled with 7042 water molecule of TIP3P. The system was neutralized by adding equivalent number of sodium ions and the system energy was minimized to 300kJ/Mol at 37°C and 1 atmosphere of pressure. The system was then equilibrated for a period of 10 nanosecond of simulation using Amber03 force filed. The equilibrated structure of DNA then transferred to Hex software installed in UBUNTU version 14.04 and blind docking were performed and the best 200 solutions were extracted and analyzed in Excel and SPSS softwares. P-value under 0.05 was used as criteria of significance throughout our analysis.

3. Results and Discussion

The acylhydrazone used in this work has been obtained from reaction of furan-2-carbohydrazide (2-furancarboxylic acid hydrazide) and benzoylacetone. Rateb et al. reported that the initial product of the condensation of benzoyl acetone and aroyl hydrazones is predominantly the enolimino form rather than the ketoenamine form and the former on cyclization gives a 5-hydroxypyrazoline derivative which may exhibit ring-chain tautomerism in solution [32]. Figure 1 show the synthesized acylhydrazone in cyclic and several chain tautomeric forms. Compound **1** was obtained as anhydrous and hydrated and both forms were characterized by X-ray diffraction analyses. The new complexes **2** and **3** were prepared by reaction of R_2SnCl_2 [R = Me (**2**) and Ph (**3**)] with hydrazone ligand in ethanol in the presence of a base to force the deprotonation of the ligand. The new complexes were characterized by elemental analysis and IR, ^{1}H, ^{13}C and ^{119}Sn NMR spectroscopy. The crystal structure of $SnMe_2L$ (**2**) has been also determined by X-ray diffraction.

3.1. Spectroscopic studies

The ligand exists exclusively in cyclic form in solid state as evidenced from comparison of its IR data with that of similar benzoylhydrazones [33] and as also confirmed from X-ray crystallography. In the IR spectrum of **1** a broad band observed at 3396 cm^{-1} has been assigned to O–H stretching vibration. Two strong bands appearing at 1640 and 1626 cm^{-1} are attributed to amido carbonyl and azomethine stretching mode, respectively. The $–CH_2–$ bending vibration is observed at 1434 cm^{-1}, and C–O stretching and O–H bending modes correspond to bands at 1318 and 1163 cm^{-1}, respectively. In the IR spectra of organotin complexes the absence of any bands attributed to ν(O-H) or ν(N-H) shows complete deprotonation of hydrazone. The lack of

absorption bands in the region 1725-1610 cm^{-1} excludes the possibility of a free or coordinated keto group in the chelated ligand. Two strong bands at 1596 and 1587 cm^{-1} in the IR spectra of both **2** and **3** have been assigned to the azometine stretching modes, ν(C=N–N=C). This low frequency for ν(C=N) is expected on coordination of nitrogen and electron delocalization in the chelate ring. The appearance of new bands in the IR spectra of the synthesized complexes assigned to ν(Sn-N) and ν(Sn-O) supports the bonding of nitrogen and oxygen to the tin atom. The presence of both ν_{sym}(Sn-C) and ν_{asym}(Sn-C) in the IR spectrum of **2** is consistent with a nonlinear C-Sn-C configuration. The IR spectra of the two complexes are in accordance with the coordination of hydrazone as a dianionic tridentate ligand via imino nitrogen and enolic oxygens corresponding to enol tautomer of hydrazone (form I, Figure 1).

The ^{1}H NMR spectrum data of **1** in $CDCl_3$ is presented in the experimental section according to the X-ray atomic numbering shown in Figure 3. This data denote that it exists exclusively in the cyclic form. The absence of any singlet signal corresponding to the methine, methylene, enol or amine protons indicate no participation of any chain tautomeric form in solution. A double doublet ($^{2}J_{HH'}$ = 18.7 Hz) at 3.00 and 3.34 ppm is attributed to two nonequivalent $-CH_2-$ protons in cyclic form. The OH proton appears as a singlet at 5.30 ppm. The aromatic and furan ring protons are observed in the region 6.55-7.63 ppm.

The ^{1}H and ^{13}CNMR data for **2** and **3** are presented in the experimental section according to the X-ray atomic numbering shown in Figure 5. In the ^{1}H NMR spectra of the two complexes, the absence of the signals corresponding to $-CH_2-$ and hydroxyl protons, and the appearance of a singlet in the range 5.66-5.83 ppm (1H) assigned to the methine proton indicate that the ligand undergoes a ring opening with complete deprotonation and coordinate to tin as enol tautomeric form I (Figure 1). The ^{1}H NMR spectrum of **2** shows a singlet for $SnMe_2$ protons surrounded by

satellites with $^{2}J(^{117/119}Sn\text{-}^{1}H)$ larger than for uncomplexed Me_2SnCl_2 ($^{2}J(^{117/119}Sn\text{-}^{1}H)$ = 65.7 / 68.7 Hz). Generally the larger coupling constant indicates the higher coordination number of tin [34]. Substitution of $^{2}J(^{119}Sn\text{-}^{1}H)$ in the Lockhart-Manders equation [35], gives a value of 129.3° for Me-Sn-Me angle in chloroform solution.

The ^{119}SnNMR spectra of complexes in noncoordinating solvent ($CDCl_3$) show one sharp singlet (-149.5 ppm for **1** and -325.1 ppm for **2**) significantly at lower frequency than that of the original Me_2SnCl_2 (+137 ppm) and Ph_2SnCl_2 (-32 ppm) which is in agreement with the increasing of coordination number of tin [34]. On the basis of the chemical shifts observed empirically for phenyltin(IV) and methyltin(IV) complexes [7-10, 36-39], the coordination number of tin for both **2** and **3** is five in $CDCl_3$.

*3.2. Crystal structures of **1** and **2***

Slow evaporation of ethanol or methanol solutions of compound **1** give single crystals of its anhydrous (**1a**) or monohydrate (**1b**) forms, respectively. The structure of the anhydrous **1a** has been reported previously [40], while the monohydrate **1b** structure is new. The crystal structure of **1b** will be discussed here in detail while the structure of **1a** will be only considered for comparison analysis. Relevant crystallographic information and selected bond distances and angles for **1b** are reported in Tables 1 and 2, respectively.

In both crystal structures (**1a** and **1b**) the ligand molecule is present in its cyclic form as also observed in solution by ^{1}H NMR spectroscopy. In the cyclic form the molecule is chiral for the presence of an asymmetric carbon atom and both anhydrous and monohydrate forms crystallize in the centrosymmetric monoclinic space group P21/c as racemic mixtures of R and S enantiomers.

The asymmetric unit of **1b** contains one ligand molecule and one water molecule and its ORTEP representation with the atomic numbering is shown in Figure 3. The more relevant differences between the two crystal structures concern the hydrogen bonding involving the molecules. The anhydrous **1a** show intermolecular hydrogen bonding between the hydroxyl group and carbonyl oxygen that led to the coupling of two adjacent molecules through a R_2^2 (4) ring (Figure 2). This pattern shows the peculiar bifurcated hydrogen bond [41] with OH…O=C of 2.04 Å (intra-) and 2.47 Å (intermolecular) observed in similar compounds [42, 43]. In **1b** the presence of a water molecule breaks the dimers (and the bifurcated hydrogen bond) and the hydroxyl group is now involved in hydrogen bonding with the crystallization water molecule, carbonyl and hydroxyl groups of adjacent molecules. Therefore one water molecule (w) participates in three different hydrogen bonds that form chains with R_4^4 (12) rings (Figure 4) with OH...O(w) 1.84 Å, OH(w)...O=C 1.93 Å , OH(w)..O(H) 2.13 Å.

The furan ring in **1a** is disordered over two positions with CH/O occupancy of 44%-56%. This fact is supported by the absence of any hydrogen bonding involving the oxygen atom of the furan ring. Disorder is also present on the methyl group with occupancy of 18%-82% . The minor component has been removed from ORTEP shown in Figure 2. Contrary to **1a,** there is no CH/O disorder of the furan ring in **1b** that, however, still continue not to be involved in hydrogen bonding. A 50%-50% disorder on the CH_3 group is present that has been removed from ORTEP shown in Figure 3. Other significant differences between the crystal structures of **1a** and **1b** are not evident. Within the pyrazoline ring of **1b** the double bond is located on the N(2)–C(8) bond (1.2786(17) Å, see Table 2 to be compared with 1.2774(16) for **1a**). The dihedral angle between

the five membered rings is 4.74(8)° in **1b** and 1.84(9)° in **1a**. The deviations from planarity is 0.002 Å (furan) and 0.033 Å (pyrazoline) in **1b** and 0.003 Å and 0.059 Å in **1a**.

Figure 5 shows an ORTEP view with the atomic numbering scheme for compound Me_2SnL (**2**). Crystallographic information and selected bond distances and angles are given in Table 2 and 3 respectively. The X-ray structural investigation confirms a ring opening with a doubly deprotonation of the ligand before to tridentately bind to tin(IV) metal atom through its ONO donor system. The tin atom is five coordinate and its coordination sphere is completed by two carbon atoms of methyl groups. The furan oxygen atom has no interaction with the tin center. To quantify the extent of distortion from ideal square pyramid (SP) or trigonal bipyramid (TBP), the index of trigonality, τ, defined by Reedijk and coworkers [44] have been used. The calculated τ value of 0.57 for **2** suggests a distorted geometry between square-pyramidal and trigonal-bipyramidal with the TBP predominating over the SP (τ = 0.0 and 1.0 are for ideal SP and TBP geometries, respectively). This distortion is mainly due to the rigidity of the six and five membered chelate rings, and is supported by the large covalent radius of tin(IV). The two methyl groups and the azomethine N(2) atom of the ligand occupy the equatorial positions of the distorted TBP while the two oxygen atoms O(2) and O(3) coordinate at the axial positions. The rigidity of the ligand impose a decrease of the O(2)-Sn-O(3) angle from the ideal value of 180° to 157.57(7)°. The two chelate 5- and 6-rings are almost planar (max deviation from the average plane of 0.007 Å) and present a dihedral angle of 5.46(8)° . In the chelate rings the distances C(5)-O(2), C(8)-O(3) and N(1)-N(2) approximate single-bond lengths whereas C(5)-N(1) and C(6)-N(2) are of order of a double bond (see Table 3) evidencing the occurrence of an electronic resonance and extensive delocalization. These observations give evidence that the ligand is coordinated according to the enol tautomeric form I (Figure 1).

The difference in the values for the C-Sn-C angle obtained from X-ray diffraction data, (120.83(15)°) and estimated in chloroform from NMR analysis (129.3°) may be related to removal of crystal network restriction in solution. The Sn–N and Sn–O bond lengths are close to the sum of the covalent radii of Sn–N (2.15 Å) and Sn–O (2.10 Å) (see Table 3). As in the structure of **1a**, the CH_3 group and the furan ring of the ligand show disorder of 20%-80% and 45%-55% occupancies, respectively. Only the major components have shown in Figure 5.

3.3. Antibacterial studies

The *in vitro* antibacterial activities of the Schiff bases and their organotin(IV) complexes were studied along with five standard antibacterial drugs, *viz*, Vancomycin, Streptomycin, penicillin, Nalidixic acid and Gentamycin. The microorganisms used in this work include *Bacillus subtilis* and *Staphylococcus aureus* (as Gram-positive bacteria) and *Escherichia coli* and *Pseudomonas aeruginosa* (as Gram-negative bacteria). The results are presented in Table 4. An inhibition zone diameter over 7 mm indicates that the ligand and its phenyltin complex are active against all bacteria under investigation [45]. Compound **1** exhibits moderate activity only in high concentration. In general the antibacterial activity of the Schiff bases may be attributed to OH and the imine group which interacts with active biological centers impairing normal cellular processes [46]. Complex **3** exhibit more inhibitory effects than the parent ligand, while almost no antibacterial effect was observed for complex **2**. More inhibitory effects of **3** than the parent ligand may be due to electron delocalization over the whole chelate ring which increases the lipophilicity of molecule (chelation theory) [45, 47-49] and also because of the biological activity effects of diphenyltin moiety. The higher activity of diphenyltin than dimethyltin complex may also be attributed to the lipophilicity increased by the presence of two phenyl

groups [50]. Generally, biological activity of organotin complexes is influenced both by donor ligand and by the number and nature of the organic groups bound to tin. The mechanism is still unknown; however, since permeability across the bacterial cell wall is necessary for the effectiveness of the biocide compounds, therefore lipophilicity is an important factor that increasing the solubility of molecule in lipids facilitates microorganism membrane crossing. With regard to the data published earlier, within the diorganotin(IV) class, the highest activity is exerted by the $[Et_2Sn(IV)]^{2+}$ and $[Ph_2Sn(IV)]^{2+}$ complexes [51]. On the other hand, di-phenyl-tin(IV) derivatives often are less toxic than other di-organo-tin(IV) derivatives [52-54]. It is interesting that **3** has remarkable activity towards *P. aeruginosa* while, the bacteria of the genus *Pseudomonas* are a group of resistant microorganism that many standard drugs were found to have no activity against it [55, 56].

3.4. DNA damage studies

The synthesized compounds have been investigated for their DNA cleavage activity by agarose gel electrophoresis method. Figure 6 represents the electrophotogram for the cleavage activity of the **1**–**3** on the isolated DNA of *B. subtilis* and *P. aeruginosa* compared to the control DNA of bacteria. The results show that **2** and **3** have no significant effects on DNA structure due to the fact that the whole genomic DNA of *B. subtilis* and *P. aeruginosa* treated with these compounds formed a sharp band in agarose well. With regard to the results of antibacterial activity (Table 4), it can be concluded that **3** can inhibit bacterial growth and multiplication by affecting bacterial cell envelope or possibly interfering with metabolic pathways whereas, it is not harmful for DNA structure. The compound **1** in this experiment had considerable destructive effects on isolated DNA of *P. aeruginosa*, while it showed no apparent inhibitory effect against corresponding

bacteria (Table 4). It may be attributed to the low permeability of this compound across the bacterial cell wall. Furthermore, because of the presence of active groups in **1**, this compound can react with active substituents present on the outer face of bacterium and deactivate them. Based on the results obtained from molecular dynamic and docking experiments (section 3.5), compound **1** can't affect gene expression in target bacteria and if it can reach DNA, will be able to bind with major groove of DNA and destruct it. While **2** and **3,** through binding with minor groove and also attachment to the upstream of genes, can disturb gene expression and consequently interfere with metabolic pathways. So, as a consequent of metabolic disorders killing of target bacteria will happen. Further complementary studies are needed to examine this hypothesis that if **2** and **3** can be used for selective gene silencing in bacterial plasmids. The absence of destructive effect on bacterial DNA can be an advantage for Ph_2SnL, hence this compound can be used safely for bacterial growth control in environment without any side effects on eukaryotic DNA. In other word, this compound will not be mutagen for eukaryotic cells.

3.5. Molecular Docking experiments

Our docking experiments indicate that the free ligand, unlike complexes, intercalates to DNA *via* its major groove and positions its hydroxy and keto groups toward N-glycosidic linkage of nucleotides and phosphordiester bonds. Because of the ligand potential to attack these bonds, the damage seen in our DNA cleavage experiments could be interpreted easily. Moreover our docking experiments also show that **2** and **3** bind strongly to DNA minor groove with hydrophobic (stacking) interactions. Analysis of 200 best solution of blind docking indicates that in 55% of solutions, compound **1** preferred to binds to regular part of DNA with binding energy

of -179.44 ± 10.02 kJ / Mol (Mean±SD), while in 12% and 33% of solutions compound **1** binds to AT and GC rich sequences of DNA respectively. This finding means that compound **1** has no effect on gene expression with any biological effects on normal or abnormal either in eukaryotic or prokaryotic cells. Our data also show that **2** and **3** preferred to bind to AT rich region from minor groove side with 68% and 72% respectively. It is well known that AT rich or TATA box (also called Goldberg-Hogness box) is a DNA sequence found in the promoter region of genes and molecules with biological effects may act with this element [57]. Binding energy for **2** and **3** to DNA string is calculated as -211.02 ± 12.5 and -236.74 ± 15.03 kJ / Mol respectively. Considering higher binding energy (p-value < 0.001) for **3** in contrast **2,** the more antibacterial effect of **3** could be easily understood.

4. Conclusion

Two new diorganotin(IV) complexes have been synthesized from reaction of diorganotin(IV) dichloride with a hydrazonic Schiff base derived from 2-furancarboxylic acid hydrazone and benzoyl acetone. On the basis of spectral and structural investigations, the Schiff base exists as cyclic form in both solution and solid phase. A novel monohydrate form of the ligand has been also obtained and structurally characterized. The ligand undergoes a ring opening reaction on complexation and coordinates to tin as tridentate dianion via imine nitrogen and enolic oxygens. The geometry of complexes is between square-pyramidal and trigonal-bipyramidal and on the basis of ^{119}Sn NMR data, coordination number of tin retains five in solution. Complex **3,** through binding with minor groove of DNA, exhibited good inhibitory effect and in view of less toxicity of diphenyltin(IV) derivatives, **3** may be a good candidate for anticancer studies. On the other

hand, due to absence of destructive effect for **3** on bacterial DNA, it can be also used safety in environment.

Acknowledgment

The authors thank Shahid Chamran University of Ahvaz (Grant No. 1393) and the Università degli Studi di Milano for financial support. DMP acknowledges the Ministry of Education and Science of Russia (Grant 14.B25.31.0005).

Appendix A. Supplementary material

CCDC 1028060, 1028061 and 1035460 contains the supplementary crystallographic data for **1a, 2 and 1b**, respectively. These data can be obtained free of charge via http://www.ccdc.cam.ac.uk/conts/retrieving.html, or from the Cambridge Crystallographic Data Centre, 12 Union Road, Cambridge CB2 1EZ, UK; fax: +44 1223 336 033; or e-mail: deposit@ccdc.cam.ac.uk.

References

[1] A.R. Katritzky, Handbook of Heterocyclic Chemistry, Pergamon, New York, 1985.

[2] S. Fustero, R. Román, J.F. Sanz-Cervera, A. Simón-Fuentes, A.C. Cuñat, S. Villanova, M. Murguía, J. Org. Chem., 73 (2008) 3523-3529.

[3] V. Valla, M. Bakola-Christianopoulou, Synth. React. Inorg. Met.-Org. Chem. , 37 (2007) 507-525.

[4] M. Rodríguez, R. Santillan, Y. López, N. Farfán, V. Barba, K. Nakatani, E.V. García Baéz, I.I. Padilla-Martínez, Supramol. Chem., 19 (2007) 641-653.

[5] A.-Z.A. Elassar, A.A. El-Khair, Tetrahedron, 59 (2003) 8463-8480.

[6] V.I. Minkin, A.V. Tsukanov, A.D. Dubonosov, V.A. Bren, J. Mol. Struct., 998 (2011) 179-191.

[7] T. Sedaghat, M. Monajjemzadeh, H. Motamedi, J. Coord. Chem., 64 (2011) 3169-3179.

[8] T. Sedaghat, M. Naseh, G. Bruno, H. Amiri Rudbari, H. Motamedi, J. Mol. Struct., 1026 (2012) 44-50.

[9] T. Sedaghat, M. Naseh, G. Bruno, H.A. Rudbari, H. Motamedi, J. Coord. Chem., 65 (2012) 1712-1723.

[10] T. Sedaghat, M. Naseh, H.R. Khavasi, H. Motamedi, Polyhedron, 33 (2012) 435-440.

[11] M. Naseh, T. Sedaghat, A. Tarassoli, E. Shakerzadeh, Comput. Theor. Chem., 1005 (2013) 53-57.

[12] M. Azarkish, T. Sedaghat, Chin. Chem. Lett., 23 (2012) 1063-1066.

[13] A.-M. Stadler, J. Harrowfield, Inorg. Chim. Acta, 362 (2009) 4298-4314.

[14] P. Dandawate, A. Ahmad, J. Deshpande, K.V. Swamy, E.M. Khan, M. Khetmalas, S. Padhye, F. Sarkar, Bioorg. Med. Chem. Lett., 24 (2014) 2900-2904.

[15] R.F. Martínez, M. Ávalos, R. Babiano, P. Cintas, M.E. Light, J.L. Jiménez, J.C. Palacios, Tetrahedron, 70 (2014) 2319-2329.

[16] E. López-Torres, F. Zani, M.A. Mendiola, J. Inorg. Biochem., 105 (2011) 600-608.

[17] H. Yin, J. Li, M. Hong, J. Cui, L. Dong, Q. Zhang, J. Mol. Struct., 985 (2011) 261-269.

[18] T. Sedaghat, M. Yousefi, G. Bruno, H. Amiri Rudbari, H. Motamedi, V. Nobakht, Polyhedron, 79 (2014) 88-96.

[19] A. Bacchi, A. Bonardi, M. Carcelli, P. Mazza, P. Pelagatti, C. Pelizzi, G. Pelizzi, C. Solinas, F. Zani, J. Inorg. Biochem., 69 (1998) 101-112.

[20] T. Sedaghat, L. Tahmasbi, H. Motamedi, R. Reyes-Martinez, D. Morales-Morales, J. Coord. Chem., 66 (2013) 712-724.

[21] T. Sedaghat, M. Aminian, G. Bruno, H. Amiri Rudbari, J. Organomet. Chem., 737 (2013) 26-31.

[22] F. Wang, H. Yin, J. Cui, Y. Zhang, H. Geng, M. Hong, J. Organomet. Chem., 759 (2014) 83-91.

[23] K.T. Mahmudov, M.F.C. Guedes da Silva, M.N. Kopylovich, A.R. Fernandes, A. Silva, A. Mizar, A.J.L. Pombeiro, J. Organomet. Chem., 760 (2014) 67-73.

[24] D. Kumar Dey, A. Lycka, S. Mitra, G.M. Rosair, J. Organomet. Chem., 689 (2004) 88-95.

[25] M.A. Affan, I. Foo, B. Fasihuddin, E. Simi, M. Hapipah, Malaysian J. Anal. Sci, 13 (2009) 73-85.

[26] M.A. Affan, N.B. Sam, F.B. Ahmad, F. White, E.R. Tiekink, Acta Crystallogr. Sect. E: Struct. Rep., 67 (2011) m965-m965.

[27] M.A. Affan, N.B. Sam, F.B. Ahmad, F. White, E.R. Tiekink, Acta Crystallogr., Sect. E: Struct. Rep., 67 (2011) m963-m964.

[28] G.F. De Sousa, E. Garcia, C.C. Gatto, I.S. Resck, V.M. Deflon, J.D. Ardisson, J. Mol. Struct., 981 (2010) 46-53.

[29] G.M. Sheldrick, Acta Crystallogr., Sect. A: Found. Crystallogr., 64 (2008) 112-122.

[30] J. Vandepitte, J. Verhaegen, K. Engbaek, P. Rohner, P. Piot, C. Heuck, Basic laboratory procedures in clinical bacteriology, World Health Organization, 2003.

[31] J. Sambrook, E.F. Fritsch, T. Maniatis, Molecular cloning, Cold spring harbor laboratory press New York, 1989.

[32] L. Rateb, B. Azmy, M.A. Nashed, M.F. Iskander, Z. Naturforsch, B: Anorg. Chem., Org. Chem., 33B (1978) 1527-1534.

[33] K.C. Joshi, R. Bohra, B.S. Joshi, Inorg. Chem., 31 (1992) 598-603.

[34] A.G. Davies, Organotin chemistry, John Wiley & Sons, 2006.

[35] T.P. Lockhart, W.F. Manders, Inorg. Chem., 25 (1986) 892-895.

[36] T. Sedaghat, M. Aminian, H. Amiri Rudbari, G. Bruno, J. Organomet. Chem., 754 (2014) 26-31.

[37] D. Kovala-Demertzi, P. Tauridou, U. Russo, M. Gielen, Inorg. Chim. Acta, 239 (1995) 177-183.

[38] V. Barba, E. Vega, R. Luna, H. Höpfl, H.I. Beltrán, L.S. Zamudio-Rivera, J. Organomet. Chem., 692 (2007) 731-739.

[39] J. Otera, J. Organomet. Chem., 221 (1981) 57-61.

[40] H. Kargar, R. Kia, M. Moghadamm, M.N. Tahir, Acta Crystallogr., Sect. E: Struct. Rep. , 67 (2011) o367-o367.

[41] T. Steiner, Angew. Chem. Int. Ed., 41 (2002) 48-76.

[42] P. Machado, P.T. Campos, G.R. Lima, F.A. Rosa, A.F. Flores, H.G. Bonacorso, N. Zanatta, M.A. Martins, J. Mol. Struct., 917 (2009) 176-182.

[43] M.A. Martins, D.N. Moreira, C.P. Frizzo, P.T. Campos, K. Longhi, M.R. Marzari, N. Zanatta, H.G. Bonacorso, J. Mol. Struct., 969 (2010) 111-119.

[44] A.W. Addison, T.N. Rao, J. Reedijk, J. van Rijn, G.C. Verschoor, J. Chem. Soc., Dalton Trans., (1984) 1349-1356.

[45] M.S. Refat, I.M. El-Deen, Z.M. Anwer, S. El-Ghol, J. Mol. Struct., 920 (2009) 149-162.

[46] W. Rehman, M.K. Baloch, A. Badshah, Eur. J. Med. Chem., 43 (2008) 2380-2385.

[47] R.V. Singh, P. Chaudhary, S. Chauhan, M. Swami, Spectrochim. Acta, Part A, 72 (2009) 260-268.

[48] M.T. Kaczmarek, R. Jastrząb, E. Hołderna-Kędzia, W. Radecka-Paryzek, Inorg. Chim. Acta, 362 (2009) 3127-3133.

[49] M.V. Angelusiu, S.-F. Barbuceanu, C. Draghici, G.L. Almajan, Eur. J. Med. Chem., 45 (2010) 2055-2062.

[50] T.S. Basu Baul, Appl. Organomet. Chem., 22 (2008) 195-204.

[51] C. Pellerito, L. Nagy, L. Pellerito, A. Szorcsik, J. Organomet. Chem., 691 (2006) 1733-1747.

[52] H.I. Beltrán, C. Damian-Zea, S. Hernández-Ortega, A. Nieto-Camacho, M.T. Ramı´rez-Apan, J. Inorg. Biochem., 101 (2007) 1070-1085.

[53] A. Olżyńska, M. Przybyło, J. Gabrielska, Z. Trela, S. Przestalski, M. Langner, Appl. Organomet. Chem., 19 (2005) 1073-1078.

[54] B. Różycka-Roszak, H. Pruchnik, E. Kamiński, Appl. Organomet. Chem., 14 (2000) 465-472.

[55] R. Juan-Luis, F. Alian, Pseudomonas, Virulence and gene regulation, Springer, 2007.

[56] D.M. Livermore, Clin. Infect. Dis., 34 (2002) 634-640.

[57] C. Yang, E. Bolotin, T. Jiang, F.M. Sladek, E. Martinez, Gene, 389 (2007) 52-65.

Figure 1. Tautomeric forms for **1**

Figure 2. An ORTEP view with a representation of intra- and intermolecular hydrogen bonds and formation of $R_2^2(4)$ ring in **1a**

Figure 3. An ORTEP view with the atomic numbering scheme for **1b**

Figure 4. A representation of intermolecular hydrogen bonds and formation of a $R_4^4(12)$ ring in **1b**.

Figure 5. An ORTEP view with the atomic numbering scheme for **2**

Figure 6. The electrophotogram for the DNA cleavage activity of the **1**–**3**. M = DNA ladder (1kb), 1 = **2** + *B. subtilis* DNA, 2 = **2** + *P. aeruginosa* DNA, 3 = **1** + *B. subtilis* DNA , 4 = **1** + *P. aeruginosa* DNA, 5 = **3** + *B. subtilis* DNA , 6 = **3** + *P. aeruginosa* DNA, 7 = *B. subtilis* DNA + H_2O_2, 8 = *P. aeruginosa* DNA + H_2O_2, 9 = unreacted DNA of *B. subtilis*, 10 = unreacted DNA of *P. aeruginosa*

Table 1 Crystallographic and structure refinement data for **1b** and **2**

Table 2. Selected bond lengths (Å), bond angles (°) and torsion angles (°) for **1b**

Table 3. Selected bond lengths (Å), bond angles (°) and torsion angles (°) for **2**

Table 4 Antibacterial activity data of ligand and its organotin(IV) complexes

Figure(s)

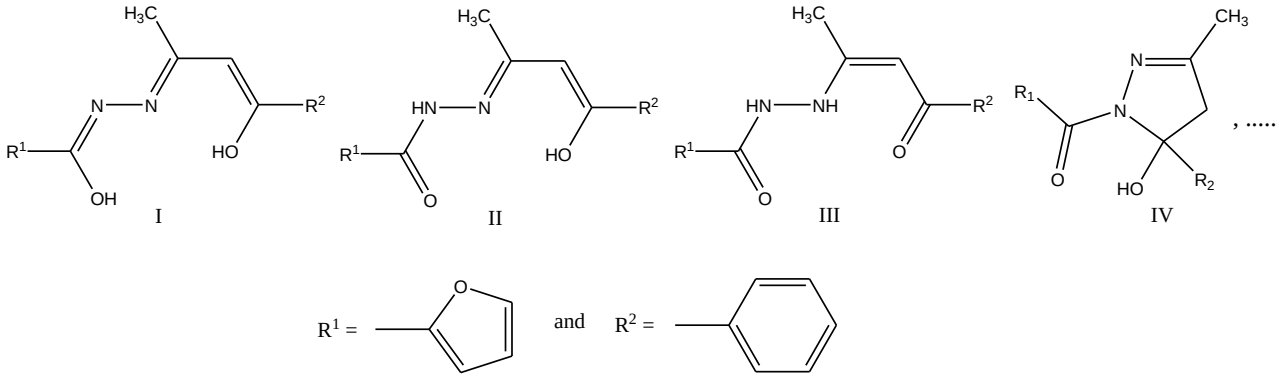

Figure 1. Tautomeric forms for **1**

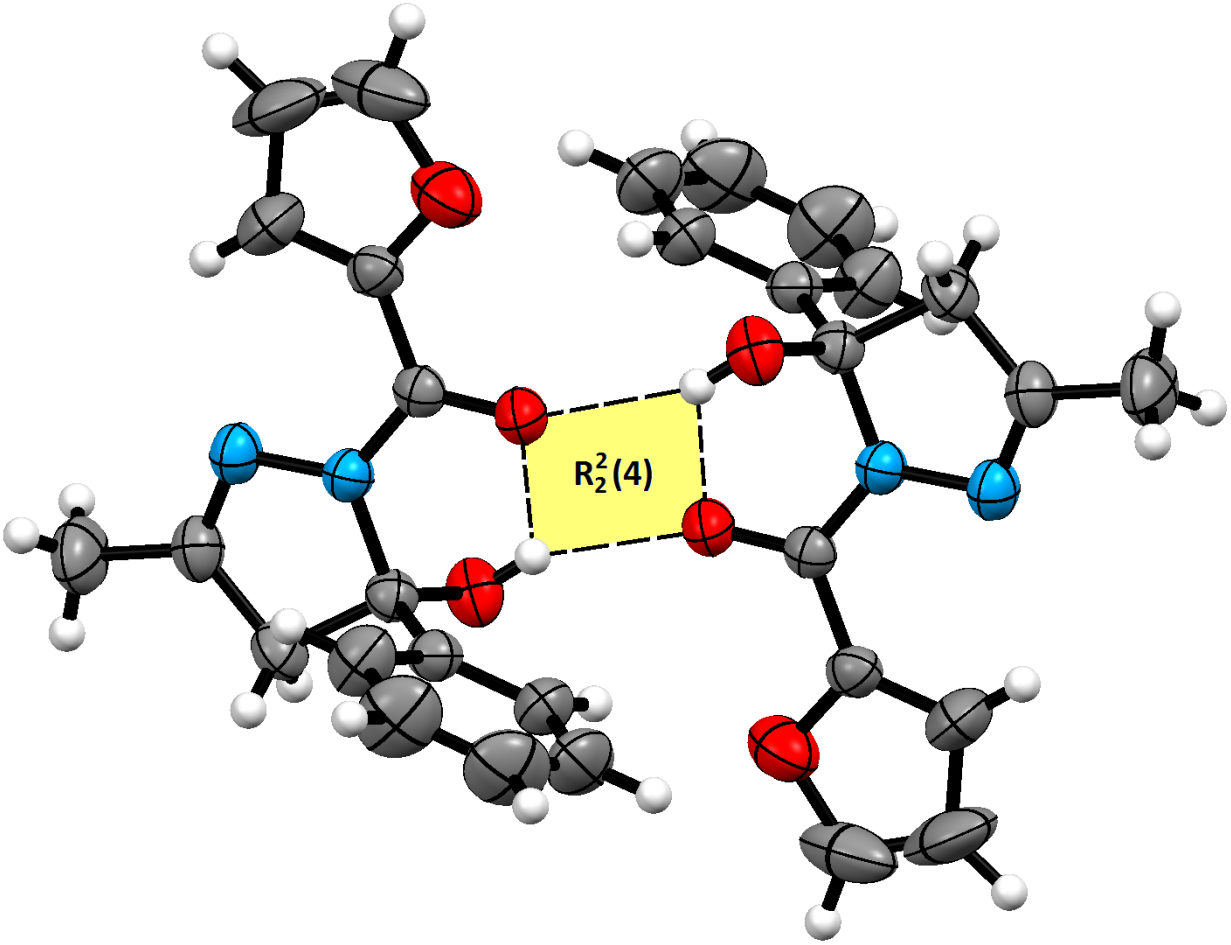

Figure 2. An ORTEP view with a representation of intra- and intermolecular hydrogen bonds and formation of $R_2^2(4)$ ring in **1a**

Figure(s)

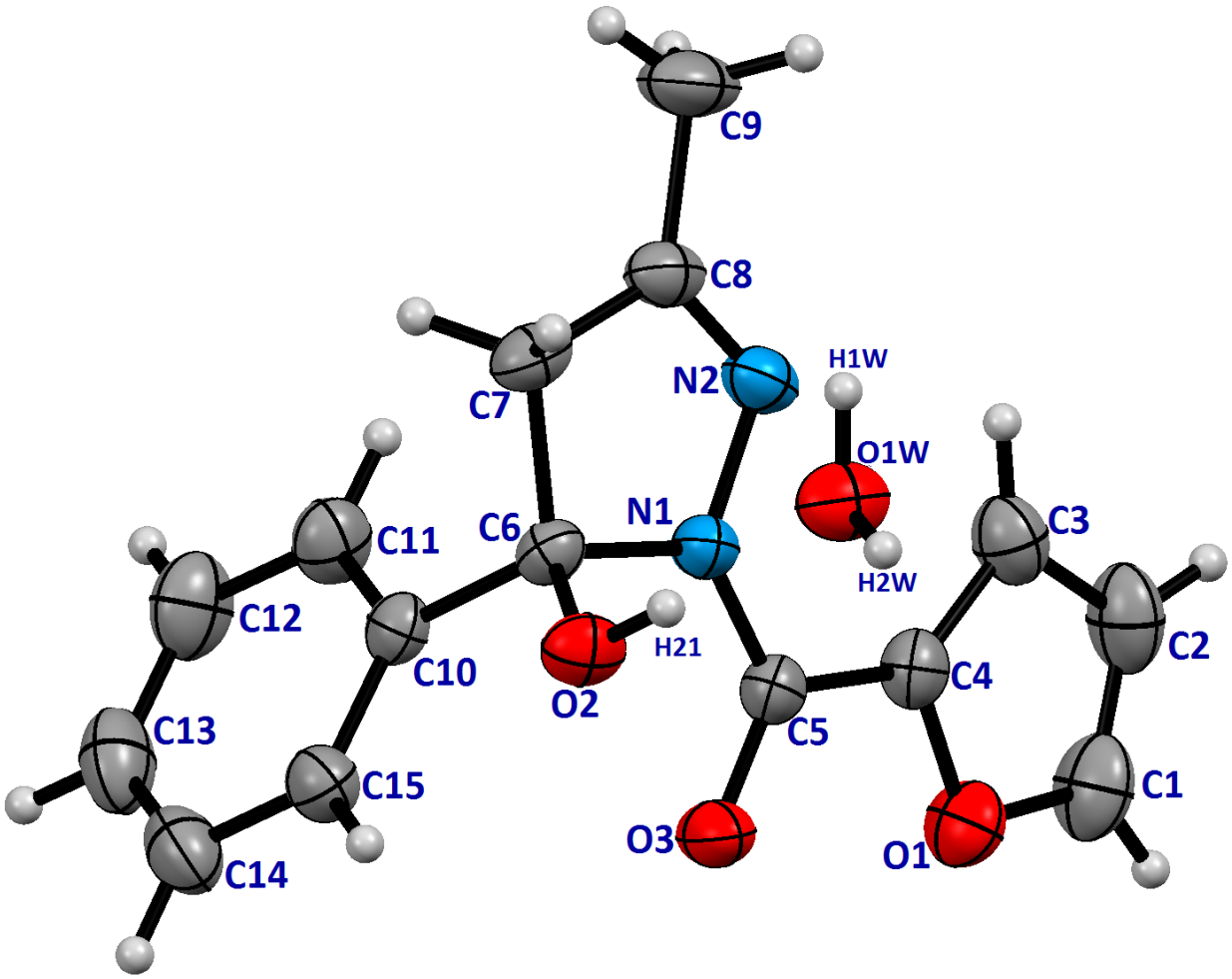

Figure 3. An ORTEP view with the atomic numbering scheme for **1b**

Figure(s)

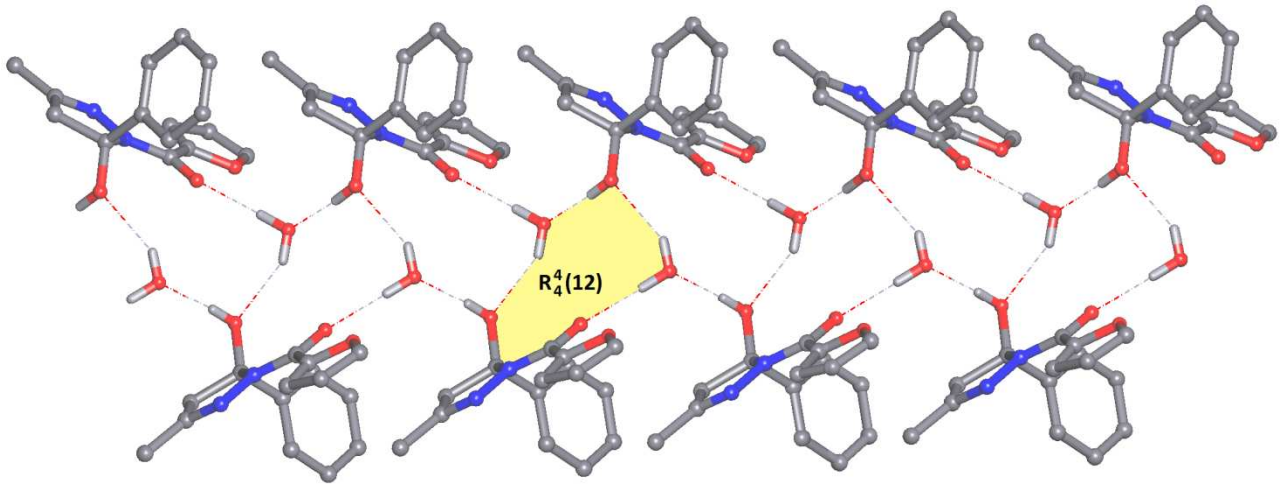

Figure 4. A representation of intermolecular hydrogen bonds and formation of a R_4^4 (12) ring in **1b**.

Figure(s)

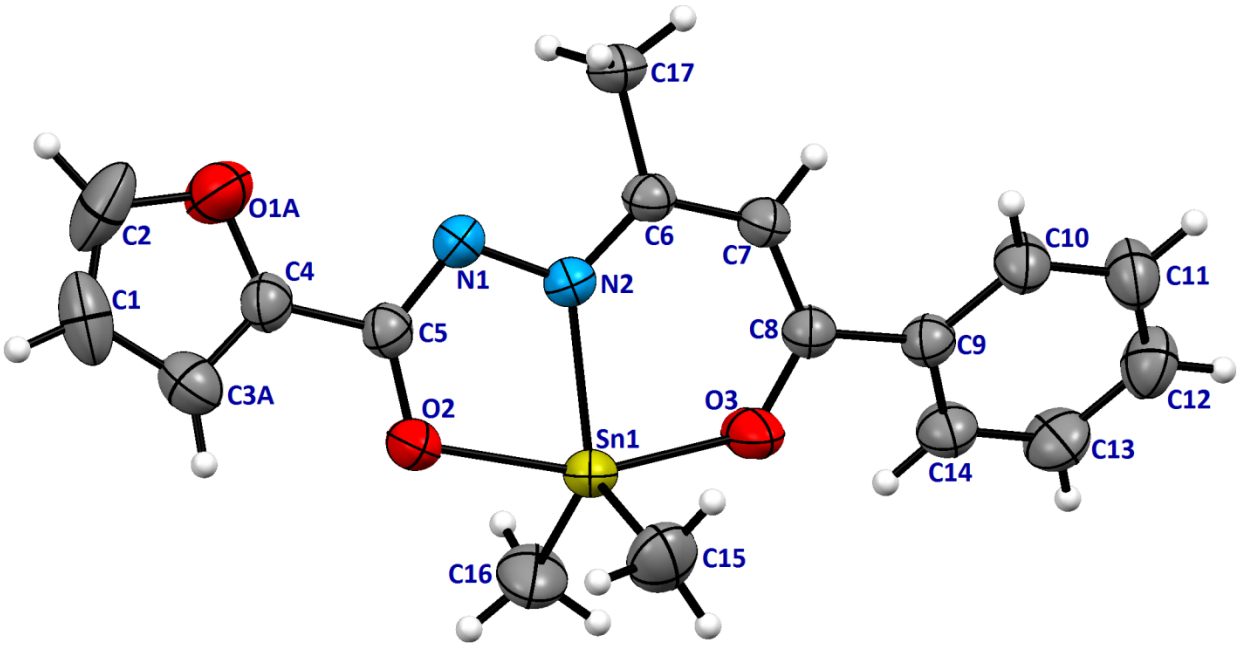

Figure 5. An ORTEP view with the atomic numbering scheme for **2**

Figure(s)

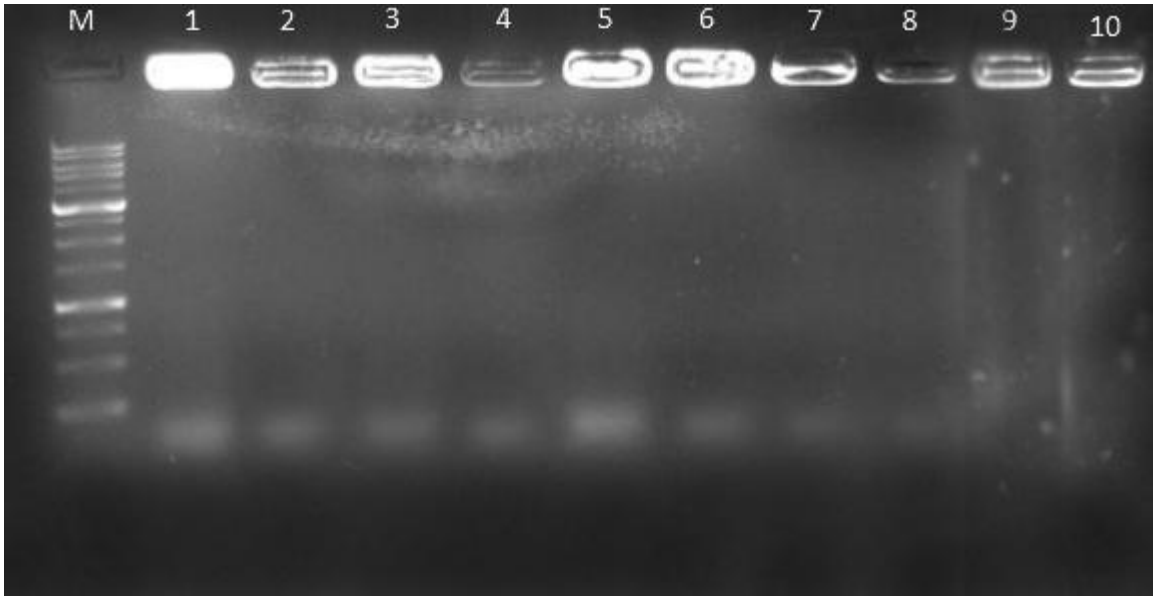

Figure 6. The electrophotogram for the DNA cleavage activity of the **1**–**3**. M = DNA ladder (1kb), 1 = **2** + *B. subtilis* DNA, 2 = **2** + *P. aeruginosa* DNA, 3 = **1** + *B. subtilis* DNA , 4 = **1** + *P. aeruginosa* DNA, 5 = **3** + *B. subtilis* DNA , 6 = **3** + *P. aeruginosa* DNA, 7 = *B. subtilis* DNA + H_2O_2, 8 = *P. aeruginosa* DNA + H_2O_2, 9 = unreacted DNA of *B. subtilis*, 10 = unreacted DNA of *P. aeruginosa*

Table(s)

Table 1 Crystallographic and structure refinement data for **1b** and **2**

	1b	**2**
Empirical formula	$C_{15}H_{16}N_2O_4$	$C_{17}H_{18}N_2O_3Sn$
Formula weight	288.30	417.02
T (K)	293(2)	293(2)
Wavelength, λ (Å)	0.71073 A	0.71073 A
Crystal system	Monoclinic	Monoclinic
Space group	*P* $2_1/c$	*P* $2_1/c$
a (Å)	12.6310(15)	11.767(7)
b (Å)	6.8000(8)	7.823(5)
c (Å)	17.143(2)	19.180(12)
α (˚)	90.00	90.00
β (˚)	105.063(2)	100.084(8)
γ (˚)	90.00	90.00
Volume ($Å^3$)	1421.8(3)	1738.3(19)
Z	4	4
$D_{calc.}$ (Mg m^{-3})	1.347	1.593
θ Ranges for data collection (˚)	1.670 to 31.605	1.758 to 31.564
F(000)	608	832
Crystal size (mm)	0.20 x 0.30 x 0.34	0.40 x 0.40 x 0.24
Absorption coefficient (mm^{-1})	0.099	1.485
Index ranges	-18<=h<=18 -10<=k<=10 -25<=l<=25	-17<=h<=17 -11<=k<=11 -27<=l<=28
Reflections collected / unique	30465 / 4472 [R(int) = 0.0223]	38642 / 5525 [R(int) = 0.0197]
Data / restraints / parameters	4472 / 0 / 198	5525 / 0 / 210
Goodness-of-fit on F^2	1.098	1.177
Final R indices [I>2σ(I)]	R_1 = 0.0494 wR_2 = 0.1390	R_1 = 0.0280 wR_2 = 0.0773
R indices (all data)	R_1 = 0.0604 wR_2 = 0.1537	R_1 = 0.0327 wR_2 = 0.0891
Largest diff. peak and hole ($e.A^{-3}$)	0.414 and -0.336	0.751 and -0.889

Table(s)

Table 2. Selected bond lengths (Å), bond angles (°) and torsion angles (°) for **1b**

C(6)–N(1)	1.5050(15)
C(6)–O(2)	1.3923(15)
C(6)–C(7)	1.5475(17)
C(6)–C(10)	1.5216(16)
N(1)–N(2)	1.3926(14)
N(1)–C(5)	1.3562(16)
O(3)–C(5)	1.2327(15)
N(2)–C(8)	1.2786(17)
C(5)–C(4)	1.4740(17)
C(7)–C(8)	1.4906(19)
C(8)–C(9)	1.491(2)
N(1)- C(6)- O(2)	111.59(9)
N(1)- C(6)- C(7)	99.77(9)
C(6)- N(1)- N(2)	113.37(9)
N(2)- N(1)- C(5)	122.89(10)
N(1)- N(2)- C(8)	108.03(10)
N(1)- C(5)- O(3)	119.9(1)
N(1)- C(5)- C(4)	119.21(10)
C(6)- C(7)- C(8)	103.83(10)
N(2)- C(8)- C(7)	114.78(11)
N(2)- C(8)- C(9)	121.22(13)
C(7)-C(6)-N(1)-N(2)	-4.31(12)
N(1)-C(6)-C(7)-C(8)	4.35(11)
C(6)-N(1)-N(2)-C(8)	2.35(14)
N(1)-N(2)-C(8)-C(7)	0.98(15)
C(6)-C(7)-C(8)-N(2)	-3.68(15)
O(1)W-H(1)W .. O(3)	2.7758(15)
O(1)W-H(2)W .. O(2)	2.8713(15)
O(2)-H(21) .. O(1)W	2.6597(15)

Table(s)

Table 3. Selected bond lengths (Å), bond angles (°) and torsion angles (°) for **2**

Sn(1)-N(2)	2.156(2)	N(2)-N(1)	1.405(2)
Sn(1)-O(2)	2.1352(19)	C(6)-C(7)	1.424(3)
Sn(1)-O(3)	2.107(2)	N(1)-C(5)	1.306(3)
Sn(1)-C(15)	2.123(3)	C(8)-C(7)	1.380(3)
Sn(1)-C(16)	2.124(3)	C(8)-O(3)	1.304(3)
N(2)-C(6)	1.326(3)	O(2)-C(5)	1.311(3)
N(2)-Sn(1)-O(2)	74.40(7)	C(6)- N(2)- N(1)	115.70(17)
N(2)-Sn(1)-O(3)	84.67(7)	Sn(1)-O(2)-C(5)	112.81(13)
N(2)-Sn(1)-C(15)	115.72(12)	Sn(1)-O(3)-C(8)	130.13(15)
N(2)-Sn(1)-C(16)	123.29(2)	N(2)-C(6)-C(7)	123.13(19)
O(2)-Sn(1)-O(3)	157.57(7)	C(17)-C(6)-N(2)	119.22(18)
O(2)-Sn(1)-C(15)	97.79(11)	N(2)-N(1)-C(5)	111.25(18)
O(2)-Sn(1)-C(16)	93.72(11)	N(1)-C(5)-O(2)	125.83(19)
O(3)-Sn(1)-C(15)	98.51(12)	N(1)-C(5)-C(4)	117.7(2)
O(3)-Sn(1)-C(16)	91.06(12)	C(9)-C(8)-O(3)	114.56(18)
C(15)-Sn(1)-C(16)	120.83(15)	C(7)-C(8)-O(3)	124.72(19)
Sn(1)-N(2)-C(6)	128.57(14)	C(6)-C(7)-C(8)	127.63(19)
Sn(1)-N(2)-N(1)	115.70(13)		
N(2)-N(1)-C(5)-O(2)	1.3(6)	N(2)-Sn(1)-O(3)-C(8)	11.2(2)
O(2)-Sn(1)-N(2)-N(1)	0.8(1)	Sn(1)-N(2)-C(6)-C(7)	5.1(3)
O(3)-Sn(1)-N(2)-C(6)	-9.5(2)	Sn(1)-N(2)-N(1)-C(5)	-1.2(2)
N(2)-C(6)-C(7)-C(8)	3.1(6)	C(7)-C(8)-O(3)-Sn(1)	-8.3(3)
O(3)-C(8)-C(7)-C(6)	-1.7(4)	Sn(1)-O(2)-C(5)-N(1)	-0.3(3)
N(2)-Sn(1)-O(2)-C(5)	-0.3(1)		

Table(s)

Table 4 Antibacterial activity data of ligand and its organotin(IV) complexes

Compound	Conc. (mg/disc)	Inhibition zone (mm)			
		E. Coli	*P. aeruginosa*	*S. aureus*	*B. subtilis*
H_2L (**1**)	3.2	11	10	11	12
	1.6	10	9	10	10
	0.8	9	8	9	9
	0.4	n.a.	7	7	n.a.
$SnMe_2L$ (**2**)	3.2	12	12	n.a.	n.a.
	1.6	n.a.	n.a.	n.a.	n.a.
	0.8	n.a.	n.a.	n.a.	n.a.
	0.4	n.a.	n.a.	n.a.	n.a.
$SnPh_2L$ (**3**)	3.2	12	22	17	21
	1.6	11	20	14	17
	0.8	10	15	12	15
	0.4	n.a.	13	11	13
Vancomycin	30	14	n.a.	17	24
Streptomycin	10	16	n.a.	12	22
Penicilin	10	12	n.a.	26	13
Nalidixic acid	30	25	n.a.	12	23
Gentamicin	10	20	20	16	21

n.a. = no activity